A Realistic Channel Model for Molecular Communication with Imperfect Receivers

Na-Rae Kim,*‡ Nariman Farsad,†‡ Chan-Byoung Chae,* and Andrew W. Eckford†
*School of Integrated Technology, Yonsei University, Korea
Email: {nrkim, cbchae}@yonsei.ac.kr
†Department of Computer Science and Engineering, York University, Canada
Email: {nariman, aeckford}@cse.yorku.ca

Abstract—In this paper, we propose a realistic channel model for a table-top molecular communication platform that is capable for transmitting short text messages across a room. The observed system response for this experimental platform does not match the theoretical results in the literature. This is because many simplifying assumptions regarding the flow, the sensor, and environmental conditions, which were used in derivations of previous theoretical models do not hold in practice. Therefore, in this paper, based on experimental observations, theoretical models are modified to create more realistic channel models.

Index Terms—Nano communication networks, molecular communication, channel model, table-top molecular communication testbed, imperfect receiver.

I. INTRODUCTION

Molecular communication [1], [2], which is one of the most prominent means of communication in nanonetworks [3], enables transmission of information through chemical signalling. It is biologically inspired from natural signalling systems such as intracellular communication. Molecules, called information/messenger molecules, are generally used as carriers of information. Messages can be encoded in the different properties such as concentration [4], [5], number [6], [7], type [8], release timing [9] , and/or ratio [10] of molecules. The information-carrying molecules that are released by the transmitter can propagate through different means such as, active transport using molecular motors [11]–[13], diffusion [14]–[16], flow [7], [17], and bacteria [8], [18], [19] until they arrive at the receiver, where they are detected and the intended message is decoded.

Molecular communication has several advantages over traditional wireless communication with the most notable ones being scalability and energy efficiency. For example, in nature molecular communication is used for intra/inter-cellular communications at microscales [20], and used as pheromones for communication between the same species at macroscales [21]. Moreover, these systems consume much less energy compared to the radio based communication systems [20]. Finally, molecular communication can be biocompatible and

can be manipulated at nano or molecular scales, which makes it ideal for biomedical applications [22]. There are also many potential applications for molecular communication at macroscopic scales such as communication inside city infrastructure, and robotics communication [23].

Although molecular communication has attracted a lot of attention in the literature recently, most work have been purely theoretical with no practical implementation of a molecular communication system at either the microscale or the macroscale. In [23], however, two authors from this paper along with a coauthor, develop the first table-top platform that is capable of transporting short text messages across the room using molecular communication. This platform was purposefully designed to be inexpensive and simple such that other researchers could use it as an experimental tool. As described in Fig. 1, it is composed of a spray and a fan at the transmitter side, and a sensor that detecting the messenger molecules at the receiver. Though not in nanoscale, the platform mimics molecular communication with drift, and successfully shows feasibility of this communication scheme. Since nanoscale devices are hardly implemented for now, the table-top molecular communication testbed is a very powerful tool to demonstrate the theoretical research, and could also provide some insights on manufacturing and implementation at nanoscales.

One of the issues observed in this platform is the difference between the theoretical system response based on previous work and the observed system response. Although the exact reason for this discrepancy is not known, some likely causes can be turbulent flows, the sensor, and other environmental factors such as random flows within the room. In this work, we find new mathematical models based on experimental results, and show that the testbed's system response can be model fairly accurately with some corrections to the previously published theoretical models. By providing this theoretical framework, we bridge the gap between the theory and practice, and provide a testbed platform along with a mathematical framework. This gives researchers an access to an inexpensive platform for research, design, and experimentation.

The rest of this paper is organized as follows. Section II investigates the system model under consideration explaining details about the testbed and experimental setup. Section III and IV proposes a new mathematical model and results,
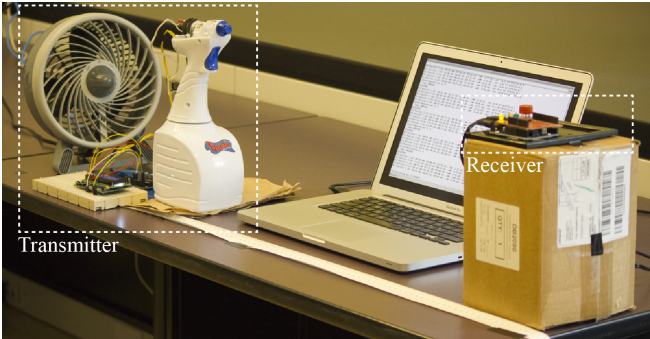
Fig. 1: A table-top testbed for molecular communication.

respectively, and we conclude the paper in Section IV.

II. EXPERIMENTAL SETUP AND PREVIOUS THEORETICAL MODELS

A. Table-Top Testbed

The macro-scale table-top testbed which is used for our experiments in this paper is shown in Fig. 1. The transmitter is composed of a spray for releasing the information molecules, a fan for assisting the propagation, and a microcontroller with an LCD display and push buttons for controlling the spray. When an input is given to the microcontroller, the information is converted into a binary stream which in turn is transmitted through controlled set of sprays. The chemical that is sprayed is isopropyl alcohol, and when the spray releases these molecules, they propagate through the medium (i.e., air) assisted by the fan behind the spray. In this work, we use two different fans, Honeywell 7 inch Personal Tech Fan, and Dyson AM01 10 inch bladeless fan, to create different flows. As shown in 3, the Dyson fan creates more laminar flows which can result in a better system response compared to the Honeywell fan. The flow speed of the wind generated by the fans, which is used in the models in this paper, is measured using Pyle PMA82 digital anemometer.

The receiver consists of an alcohol sensor and a microcontroller that reads the sensor data. Since isopropyl alcohol is used as carrier of information, MQ-3 [24] semiconducting metal-oxide gas sensor is used for detection at the receiver that detects only alcohol molecules. The microcontroller at the receiver side reads the sensor data using an analog to digital converter. The data can then be analyzed and sent to a computer through serial port. In [23], it was shown that short text messages could be transmitted across a room using this setup and on-off-keying, and that flow is required to satisfy a proper distance and data rate (bits/second). In this work, we analyze the system response of the platforms more closely, and derive theoretical models for this testbed.

The overall system response for this platform can be obtained by using a very short spray (e.g. 100 ms) at the transmitter, and measuring the sensor output at the receiver. To demonstrate this, we separate the transmitter and the receiver by 200 cm, and spray for a 100 ms. At the sensor we measure the voltage output of the sensor and record the data. We use the Dyson fan on its highest setting to generate the flow.
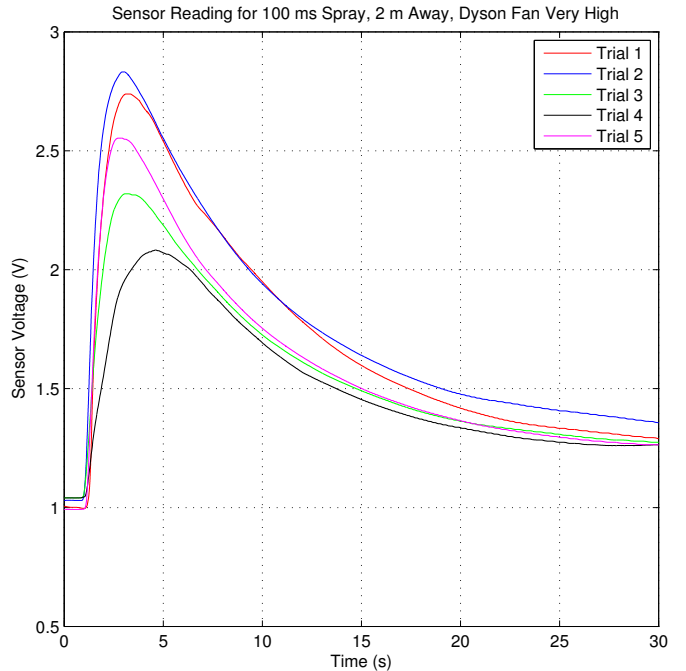

Fig. 2: The overall system response obtained experimentally.

Fig. 2 shows the system response for 5 different trials. We wait between each trial until the initial voltage reading of the sensor drops to about 1 volts. Although it is extremely difficult to find the exact cause of deviations between trials, some likely causes are: the spray, which is not precise enough to spray the same amount of alcohol for each trial; the flow, which can be turbulent; the sensor, which can be noisy; and other environmental factors such as random flows within the room.

### B. Previous Theoretical Models

We consider two theoretical models for molecular communication via diffusion assisted by drift. If we assume that the spray and the sensor have the same height in the 3 dimensional space, and that the fan's flow is perfectly aligned with the line connecting the transmitter to the receiver[1], the impulse response at the receiver should be well approximated by:

$$h_1(t) = \frac{M}{\sqrt{4\pi Dt}} \exp\Big(-\frac{(d-vt)^2}{4Dt}\Big), \qquad (1)$$

where M is the number of molecules released during the short burst, D is the diffusion coefficient, d is the separation distance between the transmitter and the receiver, v is the average flow speed from the transmitter to the receiver, and t is time. If we assume that the alcohol molecules are absorbed by the sensor upon detection, then the impulse response will be based in the inverse Gaussian distribution [17] as

$$h_2(t) = \frac{Md}{\sqrt{4\pi Dt^3}} \exp\Big(-\frac{(vt-d)^2}{4Dt}\Big). \qquad (2)$$

[1]these assumptions can be easily satisfied through careful placement of the transmitter and the receiver.
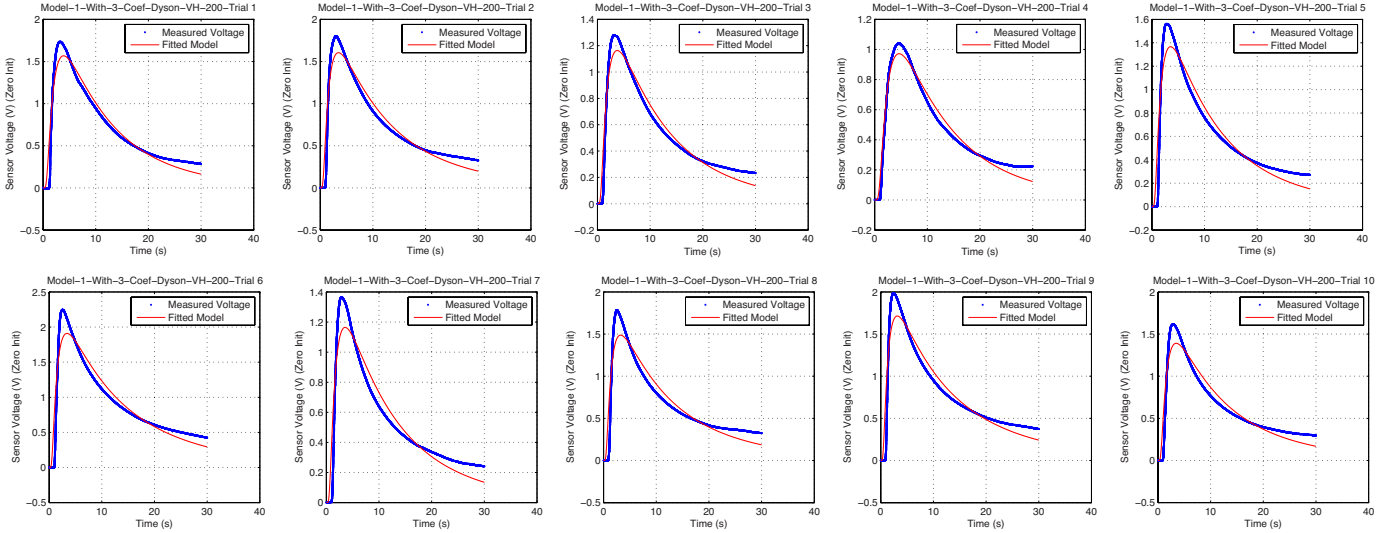
(a) A set of 10 trials, based on flows generated using the Dyson fan, are fitted with model M_1.
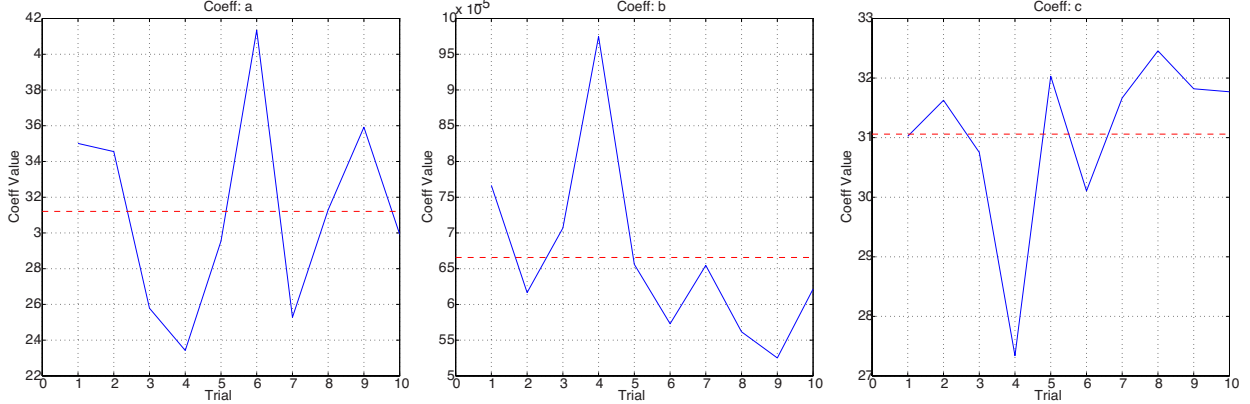
(b) The coefficients variation for 10 trials. The dashed red line is the mean value for the 10 trials.

Fig. 4: The curve fitting results.

Although the number of molecules sprayed by the transmitter is not known (in fact it is random because each spray is not perfectly and precisely similar to previous sprays), based on theoretical results, it is expected that the sensor output should have a shape similar to the curves obtained from either (1) (in case the molecules are not absorbed by the sensor) or (2) (in case they are absorbed by the sensor). Moreover, even though (1) and (2) are only applicable in one-dimensional systems, it is recently shown that three dimensional models are not different a lot [25].

C. Models versus Experimental Results

In this section we show that the theoretical models described in the previous section, do not match the experimental results obtained using the table-top platform. To demonstrate this, we separate the transmitter and the receiver by 200 cm. We then use two different fans, Honeywell 7 inch Personal Tech Fan, and Dyson AM01 10 inch bladeless fan, to create different flows. As shown in Fig. 3, the Dyson fan can create more laminar flows and can produce better system response compared to the Honeywell fan. Table I summarizes all the system parameters.

TABLE I: System Parameters.

Parameters	Values
Spraying duration for each bit	100 ms
Distance between a transmitter and a receiver	200 cm
Approximated fan speed Dyson	199 cm/s
Approximated fan speed Honeywell	192 cm/s
Diffusion coefficient of isopropyl alcohol	0.0959 cm^2/s
Temperature (room temperature)	25 °C = 298 K

If these parameters are used in the theoretical Equations (1) and (2), the system response can be calculated. Because the number of particles released by the transmitter is not known, we assume $M = 1$ and then normalize the plots by dividing them by their respective maximums. Similarly the system responses obtained from experimental results is normalized with its maximum. By normalizing the plots, we compare only the shape of the theoretical results with the shape of the experimental results. For our experimental system response, we average the response of 10 different experimental trials to produce a single plot. Moreover, the initial voltage is subtracted from the system response to effectively zero the
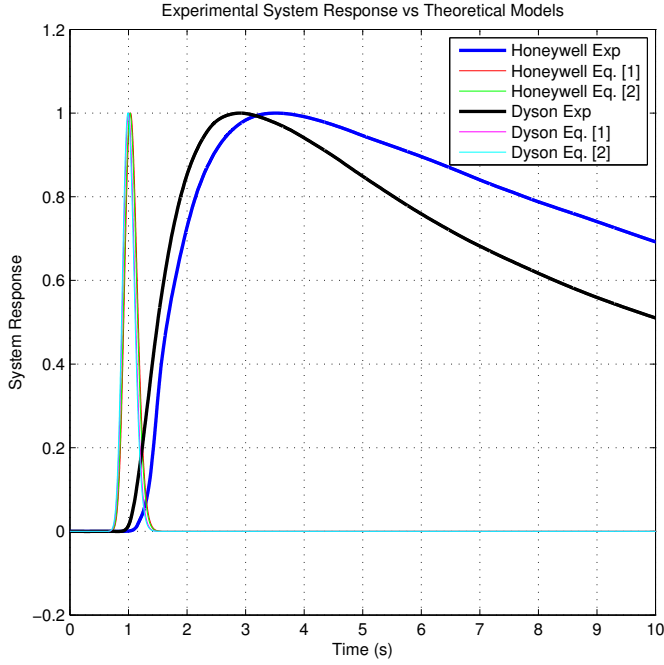
Fig. 3: Comparison of the experimental data and theoretical models from previous publications.

TABLE II: The obtained coefficients of model M_1.

Dyson on Very High				
	Mean	Variance	Variance/Mean	Mean RMSE
a	3.1208	0.3114	0.0998	
b	6.6568E-05	1.6793E-10	2.5227E-06	0.1061
c	31.0590	2.1686	0.0698	
Honeywell on High				
	Mean	Variance	Variance/Mean	Mean RMSE
a	4.6958	1.5216	0.3240	
b	8.1026E-5	1.8283E-10	2.2564E-06	0.1131
c	24.9372	10.0735	0.4040	

TABLE III: The obtained coefficients of model M_2.

Dyson on Very High				
	Mean	Variance	Variance/Mean	Mean RMSE
a	39.6950	87.4106	2.2021	
b	0.00013	4.1019E-10	3.2366E-06	0.0802
c	1.6229	9.7123	5.9845	
Honeywell on High				
	Mean	Variance	Variance/Mean	Mean RMSE
a	82.0385	1016.82	12.3945	
b	0.00016	2.5033E-10	1.5476E-06	0.1146
c	1.5452	8.9625	5.8003	

starting voltage.

Fig. 3 shows the results for both the case where the Dyson fan is used and the Honeywell fan is used. When either fans are used, the highest possible fan setting was used to generate flows. From the plot we can see that the experimental results have much wider peaks, and longer tails compared to theoretical predictions. The difference between the theoretical results and the observed system response is because of many assumptions made in derivation of the theoretical results. For example, the flow is assumed to be perfectly laminar and the sensor are assumed to be perfect at detection of concentration. These assumptions do not hold for our experimental platform. Therefore, in the rest of this paper we try to derive more realistic theoretical models based on the observed experimental data.

III. REALISTIC MODELS

In this section we use our experimental data to derive a more realistic theoretical model for our platform. First, we find likely causes of deviation from theoretical result. In particular, two system components can have a huge effect on the system response: the sensor, and the flow. The previously published channel models assume a perfectly laminar flow, and perfect and instantaneous detection at the sensor. These assumptions do not hold for our system, however.

All metal-oxide sensors, have a response time and a recovery time [26]. The response time is the time it takes for the sensor to respond to a sudden change in concentration. The recovery time is the time it takes for the sensor to drop to its initial voltage after a sudden change in concentration. Therefore, the sensor readings are expanding in time. To compensate for this effect, the system response function in

(1) and (2) must be scaled in time by a factor of α as $h_1(\alpha t)$ and $h_2(\alpha t)$, where $0 < \alpha < 1$.

Another factor that affects the system response is the flow. Previous channel models have assumed the flow to be perfectly laminar and uniform. This is, however, not the case for our platform. The high wind speeds generate turbulences with in the flow. Moreover, the Honeywell fan's blades can create pockets of air pressure that can result in more turbulent flows. Fortunately, Fick's law of diffusion can still be applied to turbulent flows with a correction term added to the diffusion coefficient [27]. Therefore, a correction must be made to the diffusion coefficient D in (1) and (2).

The final factor we consider is the flow speed. Although we measure the wind speed generated by our fans, the alcohol droplets in the spray stream, may be travelling at a slower average speed because of their weight and air friction. Therefore, a third correction is needed in (1) and (2) for the average flow velocity v.

Considering these three effects, we propose two new models based on (1) and (2),

$$M_1(t) = \frac{a}{\sqrt{t}} \exp\left(-b\frac{(d-ct)^2}{t}\right), \qquad (3)$$

$$M_2(t) = \frac{a}{\sqrt{t^3}} \exp\left(-b\frac{(ct-d)^2}{t}\right), \qquad (4)$$

where a, b, and c are corrected constants. Corrected constant a contains the scaling factor α from the sensor respond and resume times, and the correction to the diffusion coefficient because of turbulent flow. The corrected constant b contains the correction to diffusion coefficient because of turbulent flow and scaling factor α. Finally, the corrected coefficient c contains the correction to the average flow speed as well as the scaling factor α.
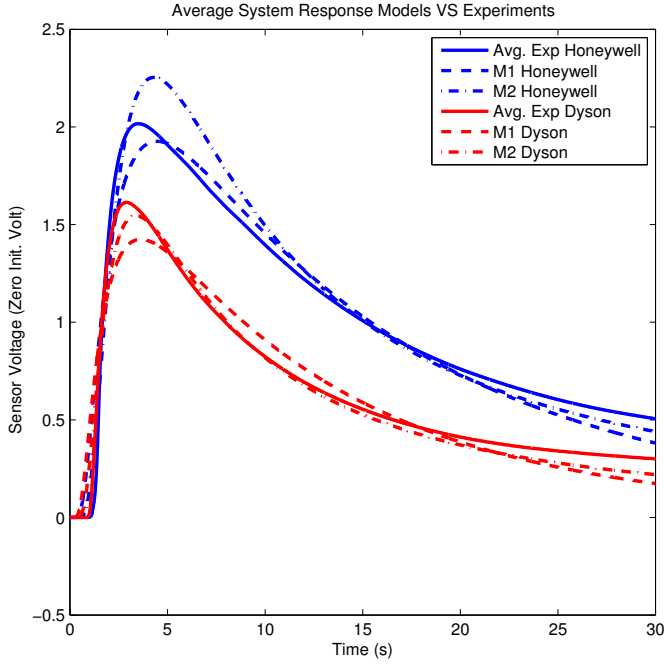
Fig. 5: Average system response of experimental observations and fitted models.

IV. RESULTS

Finding the value of these proposed corrections can be very challenging. Therefore, we use the experimental data from our platform to estimate the value of these corrections. To do this we place the transmitter and the receiver 200 cm apart. We place the sensor, the spray and the fans at the same height, with the fan blowing in the direction of the line connecting the spray to the sensor. We measure and record the overall system response to a very short spray burst of 100 ms during 10 different experimental trials.

MATLAB's curve fitting function `fit()` is then used to find the value of these three coefficients that best fits the result of each experimental trial. Fig. 4 shows the results for the case when the Dyson fan is used to generate flows, and model M_1 is used for curve fitting. In Fig. 4a, we can see that the fitted model resembles the obtained results much more accurately compared to Fig. 3. Fig. 4b shows the plot of each coefficient value for each trial. The dashed red line indicates the mean value of each coefficient.

For the goodness of fit measure, we use the root mean square error (RMSE) between the fitted model and the experimentally observed system responses. We also use the variance-to-mean ratio (VMR) as a goodness of fit measure. If this ratio is greater than 1, then the resulting coefficient is not a good fit. If this ratio is less than 1, then the coefficient is a good fit. Table II and III summarize the result for model M_1 and model M_2 given in (3) and (4), respectively. For each model the results obtained based on the Dyson fan and the Honeywell fan are presented. In the table the mean RMSE is the average RMSE across all 10 experimental trials.

From the results we can see that model M_1 is a better model when the Honeywell fan is used. When the Dyson fan is used

model M_1 has a better VMR, while model M_2 has a better RMSE. Generally, because model M_1 has lower VMR, the randomness between different trials can be modelled better through the randomness in the coefficients.

To further compare the proposed models to the experimental results, we average the system response from all 10 trials to generate the averaged experimental system response. We also use the mean of the coefficients across all 10 trials in each model to generate the corresponding system response. The results are shown in Fig. 5. Based on the results we can see that both new models capture the average system response of the testbed platform much more accurately compared to old models.

V. CONCLUSIONS

Since well-known theoretical models for molecular communication with drift do not match with experimental data, we suggest a new realistic channel model from experiments. First, we repeat the experiments with two testbeds equipped with the different kinds of fans, and perform a curve fitting session to find the best the model function to our data. Thus, we suggest a new mathematical model where proper correction factors are added to the theoretical model. For the future work, we will consider a multiple-input multiple-output case to increase achievable data rates. Eventually, prior work based on the theoretical model will be revisited with our new realistic model. For instance, in [28], we can further optimize the symbol intervals applying a new channel model.

REFERENCES

[1] S. Hiyama, Y. Moritani, T. Suda, R. Egashira, A. Enomoto, M. Moore, and T. Nakano, "Molecular communication," in *Proc. of 2005 NSTI Nanotechnology Conference*, 2005, pp. 391–394.

[2] T. Nakano, A. W. Eckford, and T. Haraguchi, *Molecular communication*, Cambridge University Press, 2013.

[3] I. F. Akyildiz, F. Brunetti, and C. Blazquez, "Nanonetworks: A new communication paradigm," *Computer Networks*, vol. 52, no. 12, pp. 2260–2279, 2008.

[4] M. U. Mahfuz, D. Makrakis, and H. T. Mouftah, "On the characterization of binary concentration-encoded molecular communication in nanonetworks," *Nano Communication Networks*, vol. 1, no. 4, pp. 289–300, 2010.

[5] M. S. Kuran, H. B. Yilmaz, T. Tugcu, and I. F. Akyildiz, "Modulation techniques for communication via diffusion in nanonetworks," *Proc. IEEE Int. Conf. on Comm.*, June 2011.

[6] N. Farsad, A. W. Eckford, S. Hiyama, and Y. Moritani, "Quick system design of vesicle-based active transport molecular communication by using a simple transport model," *Nano Communication Networks*, vol. 2, no. 4, pp. 175–188, 2011.

[7] N. Farsad, A. Eckford, S. Hiyama, and Y. Moritani, "On-Chip Molecular Communication: Analysis and Design," *IEEE Transactions on NanoBioscience*, vol. 11, no. 3, pp. 304–314, 2012.

[8] L. C. Cobo and I. F. Akyildiz, "Bacteria-based communication in nanonetworks," *Nano Communication Networks*, vol. 1, no. 4, pp. 244–256, 2010.

[9] A. W. Eckford, "Timing information rates for active transport molecular communication," in *Nano-Net*, vol. 20 of *Lecture Notes of the Institute for Computer Sciences, Social Informatics and Telecommunications Engineering*, pp. 24–28. Springer Berlin Heidelberg, 2009.

[10] N.-R. Kim and C.-B. Chae, "Novel modulation techniques using isomers as messenger molecules for molecular communication via diffusion," *IEEE Jour. Select. Areas in Comm.*, vol. 31, no. 12, pp. 847–856, December 2013.

[11] A. Enomoto, M. Moore, T. Nakano, R. Egashira, T. Suda, A. Kayasuga, H. Kojima, H. Sakakibara, and K. Oiwa, "A molecular communication system using a network of cytoskeletal filaments," in *Proc. of 2006 NSTI Nanotechnology Conference*, 2006, pp. 725–728.

[12] S. Hiyama, Y. Moritani, R. Gojo, S. Takeuchi, and K. Sutoh, "Biomolecular-motor-based autonomous delivery of lipid vesicles as nano- or microscale reactors on a chip," *Lab on a Chip*, vol. 10, no. 20, pp. 2741–2748, 2010.

[13] N. Farsad, A.W. Eckford, and S. Hiyama, "Modelling and design of polygon-shaped kinesin substrates for molecular communication," in *Proc. of 12th IEEE Conference on Nanotechnology (IEEE-NANO)*, Birmingham, UK, 2012, pp. 1–5.

[14] T. Nakano, T. Suda, T. Koujin, T. Haraguchi, and Y. Hiraoka, "Molecular communication through gap junction channels," *Springer Transactions on Computational Systems Biology X*, vol. 5410, pp. 81–99, 2008.

[15] M. Pierobon and I. F. Akyildiz, "A physical end-to-end model for molecular communication in nanonetworks," *IEEE Jour. Select. Areas in Comm.*, vol. 28, no. 4, pp. 602–611, May 2010.

[16] M. Pierobon and I.F. Akyildiz, "Capacity of a diffusion-based molecular communication system with channel memory and molecular noise," *IEEE Transactions on Information Theory*, vol. 59, no. 2, pp. 942–954, 2013.

[17] K. V. Srinivas, A. W. Eckford, and Raviraj S. Adve, "Molecular communication in fluid media: The additive inverse gaussian noise channel," *IEEE Trans. Info. Th.*, vol. 58, no. 7, pp. 4678–4692, July 2012.

[18] M. Gregori and I. F. Akyildiz, "A new nanonetwork architecture using flagellated bacteria and catalytic nanomotors," *IEEE Journal on Selected Areas in Communications*, vol. 28, no. 4, pp. 612–619, 2010.

[19] P. Lio and S. Balasubramaniam, "Opportunistic routing through conjugation in bacteria communication nanonetwork," *Nano Communication Networks*, vol. 3, no. 1, pp. 36–45, Mar. 2012.

[20] T. McKee and J. R. Mcfee, *Biochemisty*, Oxford University Press, 2009.

[21] W. C. Agosta, *Chemical Communication: The Language of Pheromones*, W H Freeman & Co, first edition edition, Aug. 1992.

[22] B. Atakan, O. B. Akan, and S. Balasubramaniam, "Body area nanonetworks with molecular communications in nanomedicine," *IEEE Communications Magazine*, vol. 50, no. 1, pp. 28–34, 2012.

[23] N. Farsad, W. Guo, and A. W. Eckford, "Tabletop molecular communication: Text messages through chemical signals," *PLOS ONE*, vol. 8, no. 12, December 2013.

[24] Henan Hanwei Electronics Co. Ltd. of China, *MQ3*, https://www.sparkfun.com/datasheets/Sensors/MQ-3.pdf.

[25] H. B. Yilmaz, A. C. Heren, T. Tugcu, and C.-B. Chae, "3-d channel characteristics for molecular communications with an absorbing receiver," *submitted for journal publication*.

[26] V. E. Bochenkov and G. B. Sergeev, "Sensitivity, selectivity, and stability of gas-sensitive metal-oxide nanostructures," *Metal Oxide Nanostructures and Their Applications*, pp. 31–52, 2010.

[27] A. Guha, "Transport and deposition of particles in turbulent and laminar flow," *Annual Review of Fluid Mechanics*, vol. 40, no. 1, pp. 311–341, 2008.

[28] N.-R Kim, A. W. Eckford, and C.-B. Chae, "Symbol interval optimization for molecular communication with drift," *submitted for journal publication*.